

Simultaneous measurement of saturation and relaxation in human brain by repetitive magnetization transfer pulses

Gunther Helms^{1,2*} and Andreas Piringer²

¹Section on Experimental Radiology, Department of Diagnostic Radiology, University Hospital, Tübingen, Germany

²MR Research Center, Department of Clinical Neuroscience, Karolinska Institutet, Stockholm, Sweden

Received 22 January 2004; Revised 25 June 2004; Accepted 5 August 2004

ABSTRACT: Magnetization transfer (MT) by equidistant pulse trains can be described as being analogous to progressive partial saturation, where ‘direct’ saturation of water is amplified by MT contributions that are dependent on macromolecular content and differential saturation. This concept was applied to study the transition to steady state in the human brain using similar MT-pulses as in imaging. Up to 41 bell-shaped MT-pulses of 12 ms duration were applied at frequency offsets between 0.5 and 15 kHz with flip angles between 1080 and 1440°. Central white and parietal gray matter was studied in human subjects using STEAM for localized read-out ($TE = 30$ ms, $TM = 13.7$ ms). The apparent degree of saturation, δ_{app} , and the longitudinal relaxation of the water pool during the pulse repetition period (PR) were fitted to the transient behavior after signal correction for cerebro-spinal fluid. PR was varied between 15 and 100 ms to assess the PR-dependence of the fitted parameters. The MT-term in δ_{app} exceeded the direct saturation and attained its maximum at $PR \geq 100$ ms. The macromolecular pool was only partially saturated by a single MT-pulse. The offset may be increased to 2.5 kHz to reduce direct saturation without sacrificing MT in white matter. The estimated relaxation rates (1.04 ± 0.11 s⁻¹ in WM; 0.76 ± 0.13 s⁻¹ in GM) were faster than are commonly observed at 1.5 T. The apparent saturation is a measure for MT that is not confounded by relaxation. To maximize MT in brain tissue, MT-pulses should be applied at $PR = 100$ ms or longer. At shorter PR, a larger steady state saturation is obtained at the cost of increased contributions from direct saturation. Since this accelerates the convergence, PR should be decreased to reach the steady state within a specified time. A faster transition can always be achieved at a reduced frequency offset via increased direct saturation. Copyright © 2004 John Wiley & Sons, Ltd.

KEYWORDS: magnetisation transfer; relaxation; progressive saturation; quantification; human brain

INTRODUCTION

Magnetization transfer (MT) is a contrast mechanism in tissue that is based on cross-relaxation or chemical exchange between protons in bulk water and rotationally immobilized macromolecules.^{1,2} MT experiments for clinical purposes are generally performed with a T_2 -selective radio-frequency (RF) pulse applied prior to slice excitation. This ‘MT-pulse’ specifically saturates the macromolecular magnetization, and MT is then observed as a reduction in image intensity. Its normalized value, the so-called the MT ratio (MTR), is commonly used to measure the strength of the MT effect.

The simplest multi-pulse MT experiment involves a long train of identical MT pulses followed by a single-shot sequence to read out the partially saturated polariza-

tion. This allows application of shorter pulse repetition periods (PR) than in interleaved saturation–acquisition schemes, and the use of pulses of higher power without violating specific-absorption-rate limits. This approach has been used to replace continuous wave (CW) irradiation of RF power in humans.^{3–6} Such schemes also simplify quantification of the exchange kinetics,^{7,8} since the transfer is not disturbed by the read-out after an MT-pulse has been applied. We recently presented solutions in closed form for the dynamic and stationary behavior.^{9,10}

Increased water content normally results in slower longitudinal relaxation and reduced MT. These effects amplify each other transiently; however, they partially cancel each other in the steady state. The observation that similar steady-state MTRs were found in gray and white matter of human brain (GM, WM)¹⁰ may be regarded as a fundamental limitation of using trains of MT pulses. From the theory we derived an approximation that describes the measured signals in the same way as partial progressive saturation of a liquid. This makes it possible to determine two different parameters from the transition to the steady state: the longitudinal relaxation during PR

*Correspondence to: G. Helms, MR Forschung in der Neurologie und Psychiatrie, Universitätsklinikum Göttingen, Robert-Koch-Str. 40, DE-37075 Göttingen, Germany.

E-mail: ghelms@gwdg.de and gunther.helms@cns.ki.se

Abbreviations used: CSF, cerebro-spinal fluid; CW, continuous wave; GM, gray matter; MT, magnetization transfer; MTR, magnetization transfer ratio; PR, repetition period of saturation; RF, radio frequency; STEAM, stimulated echo acquisition mode; WM, white matter.

and the apparent degree of saturation. The latter describes how the direct saturation created by one pulse is increased by MT until the next pulse is applied. One may thus obtain parameters representing solely relaxation or saturation, to avoid confounding MT and relaxation in the steady-state MTR.

In this *in vivo* study, we applied this approach to investigate MT in white and gray matter in human brain tissue using single-volume localization. In particular, the dependence of the dynamic behavior on PR, pulse power and frequency offset was studied. We also derived a simple formula to describe the transition in terms of time. This immediately suggested a strategy to ensure convergence onto the steady state under conditions where the number of pulses and the total preparation time are limited.

THEORY

The term progressive partial saturation refers to an experiment in which the polarization is saturated by repetitive RF pulses of a flip angle smaller than 90° . Both the transient and stationary behavior depend on the degree of saturation and the relaxation between consecutive pulses. The standard binary spin-bath model of MT considers the pools of 'free' bulk water and of motion-restricted 'macromolecules' (denoted by subscripts 'f' and 'm', respectively), thus extending the elementary notion describing tissue as a homogeneous liquid. Our description will be limited to longitudinal magnetization and relaxation rates (R_{1f} , R_{1m}), so the subscript 'z' is omitted. In equilibrium, the magnetization of the pools (M_f^0 , M_m^0) is balanced by the respective pseudo first-order rate constants k_{fm} and k_{mf} . Therefore, the macromolecular fraction, F , can be expressed by the rate constants:

$$F = M_m^0 / (M_f^0 + M_m^0) = k_{fm} / (k_{fm} + k_{mf}) \quad (1)$$

The evolution of polarization between two MT pulses can be approximated by an initial fast transfer restoring the kinetic equilibrium and a slow relaxation to thermodynamic equilibrium because the difference in relaxation during the transfer time is small in tissues ($R_{1m} - R_{1f} \ll k_{fm} + k_{mf}$).⁹ The apparent rate of the transfer is

$$\lambda_T = k_{fm} + k_{mf} + (1 - F)R_{1m} + FR_{1f} \quad (2)$$

and

$$\lambda_R = (1 - F)R_{1f} + FR_{1m} \quad (3)$$

is the relaxation rate that is observed in pulsed MT experiments.⁹ R_{1m} cannot be determined reliably if the experimental error of λ_R is of the order of F . Since F is small, $R_{1m} = 1 \text{ s}^{-1}$ can safely be assumed in quantitative

CW studies without affecting the results. For pulsed MT, a suitable approximation is $\lambda_R \approx R_{1f}$.⁹

The RF absorption properties of the pools (individual absorption line shapes) are not taken into account here. Instead, the effect of a single saturation pulse on each pool is described by a specific degree of saturation, δ_f and δ_m . It is also assumed that the saturation pulses act instantaneously, and that exchange and relaxation take place during the entire pulse repetition period without interference with the applied MT pulse.^{11,12} In order to describe the dynamic behavior of the observable water in analogy to progressive partial saturation of a homogeneous liquid, the apparent saturation of the water pool is defined as

$$\delta_{app} = \delta_f + F(\delta_m - \delta_f) \frac{1 - E_T/E_R}{1 - (1 - \delta_m)E_T} \quad (4)$$

Here, $E_{T/R} = \exp(-\lambda_{T/R} \text{ PR})$ denotes the exponential of transfer and relaxation during PR. The apparent saturation contains a constant term of direct saturation and a PR-dependent term of MT that is proportional to the macromolecular fraction and to the differential saturation. When the transfer is fully accomplished, δ_{app} assumes a constant maximum at long PR $\gg 1/\lambda_T$:

$$\delta_{eq} = (1 - F)\delta_f + F\delta_m \quad (5)$$

The weighting by the relative pool size indicates that the kinetic equilibrium between the partially saturated pools has been re-established before the next MT pulse is applied. In this case, the free water is described by the weighted averages [eqns (3) and (5) replace R_{1f} and δ_f]. Using δ_{app} , the saturated signal after n MT-pulses is written as:

$$S(n) = S(0) \left[\frac{1 - E_R}{1 - (1 - \delta_{app})E_R} + \frac{\delta_{app}E_R}{1 - (1 - \delta_{app})E_R} \times [(1 - \delta_{app})E_R]^n \right] \quad (6)$$

This equation may be used to fit relaxation and apparent saturation (including MT). The representation in terms of time, $t = \text{PR } n$, may be more familiar because it is commonly used to describe CW saturation:

$$S(n) = S(0)[1 - \text{MTR} + \text{MTR} \exp(-R_{app} \text{ PR} n)] \quad (7)$$

Here, MTR is the steady state saturation,

$$\text{MTR} = \frac{\delta_{app}E_R}{1 - (1 - \delta_{app})E_R} \quad (8)$$

and R_{app} is the apparent rate of the transition,

$$R_{app} = \lambda_R - \frac{\ln(1 - \delta_{app})}{\text{PR}} \cong \lambda_R + \frac{\delta_{app}}{\text{PR}} \quad (9)$$

The linear expansion requires that $\delta_{\text{app}} \ll 1$, i.e. a small direct saturation and a low macromolecular content. These conditions are usually met in MT experiments. Thus, the transition rate is amplified by periodical saturation. Once δ_{eq} has been attained, the PR-dependence of R_{app} is

$$R_{\text{app}} \cong \lambda_{\text{R}} + \frac{\delta_{\text{eq}}}{\text{PR}} \quad (10)$$

For increasing PR, the apparent transition rate slowly approaches its lower limit, the apparent relaxation rate.

METHODS

The study was performed on a 1.5 T clinical MR system (Signa Advantage, 5.4.3 software level, General Electric Medical Systems, Milwaukee, WI, USA) equipped with a 10 mT/m gradient system. The standard headcoil, a 28 cm birdcage resonator, was used. The experiments were performed on healthy adult volunteers in accordance with the Helsinki convention as supervised by the local ethics review board.

The motion-restricted magnetization was saturated by a train of equidistant band-selective RF pulses. The duration of the pulse train was limited to times shorter than 1.6 s. Thus, the transition to steady state had to be adjusted to these system restrictions. ‘Bell-shaped’ pulses [hamming-filtered main-lobe of the $\sin(x)/x$ function] were used because of their small time–bandwidth product and high power integral. The highest saturation was achieved with pulses of 12 ms duration. Thus, maximum flip angles between 1450 and 1500°, and up to 41 pulses of 1440° could be applied, depending on the RF load. Short MT pulses (6 ms) yielded inferior integral power (\propto flip angle²/pulse length) due to system restrictions on the peak amplitude. Restrictions on the accumulated pulse duration reduced the number of MT pulses when the duration was increased to 24 ms. The attenuated water signal was then read out with single-volume localization by the stimulated echo acquisition mode¹³ (STEAM, $TE = 30$ ms, $TM = 13.7$ ms). The MT pulses were implemented into the manufacturer’s STEAMCSI sequence by modifying the water suppression part of the sequence.¹⁴ The direction of the ‘spoiler’ gradients was permuted to dephase residual coherent transverse magnetization.

The ‘trade-off’ between high saturation of macromolecules vs unwanted direct saturation of free water depends mainly on the frequency offset. The direct saturation was measured in a phantom containing a solution of MnCl_2 with similar relaxation times as in WM ($T_1 = 630$ ms, $T_2 = 73$ ms, measured by varying TR and TE of the STEAM sequence). The saturation profile of the MT pulse train was measured by applying a constant gradient during pulse train and acquisition.

The saturated signal was then subtracted from a reference acquisition. These frequency offsets were chosen to be outside the central frequency band of direct excitation of coherent transverse magnetization, which is characterized by spikes occurring periodically at reciprocal PR in the profile of direct saturation.⁴ Outside this band, the liquid pool M_f is saturated by absorption of RF energy in a similar way as for CW irradiation.¹⁵ The direct saturation of the MT pulses at 0.5, 0.75, 1, 1.5 and 2 kHz offset was estimated by fitting eqn (6) to the transition. The resulting saturations were identical whether gradient spoiling was performed or not. Apparently, no detectable transverse magnetization is created due to the adiabatic behavior of the smooth selective pulses.¹⁵

In vivo, the transition was measured for five to eight values of a PR between 15 and 100 ms, depending on the examination time and volunteer compliance. One pulse parameter was changed to study its influence on the transient behavior. The nominal flip angle was chosen between 1080 and 1440° in order to generate a distinct MT effect within 1.6 s. These MT pulses had higher power than those commonly applied in MT imaging protocols.¹⁶ To avoid excessive direct saturation the frequency offset was chosen between 1 and 3 kHz (see Results). Volumes were localized in the centrum semiovale containing only WM, and across the central fissure containing mainly parietal GM from both cortical hemispheres. Signal contributions from cerebro-spinal fluid (CSF) to GM voxels of interest (VOIs) were determined by increasing TE in 12 geometric steps from 30 to 2000 ms and fitting two exponential relaxation components as described previously.⁵ The CSF signal fraction at $TE = 30$ ms was calculated from the components, and then subtracted to yield the tissue signal.

Reference measurements were performed with a flip angle of zero for each transition to account for slow signal variation due to system instability and subject movement. These points were included in the data at $n = 0$ for before fitting eqn (6) to estimate δ_{app} and E_{R} . The apparent transition rate and MTR were determined individually for each value of PR from eqn (7). The apparent longitudinal relaxation time, $T_{1\text{app}} = 1/\lambda_{\text{R}}$, was derived from the PR-dependence of E_{R} in five subjects for each region:

$$E_{\text{R}}(\text{PR}) = \exp[-(\text{PR} - \Delta\text{PR})\lambda_{\text{R}}] \quad (11)$$

The parameter ΔPR was introduced to account for a potential reduction of free evolution by the RF irradiation. All samples of E_{R} obtained from the same subject were combined, but weighted with their individual standard error. Data analysis and display was performed using KaleidaGraph 3.0.5 (Abelbeck Software, Reading, PA, USA). Nonlinear least-square curve fitting was performed with numerical estimation of the derivatives as implemented in KaleidaGraph.

RESULTS

The dependence of the transition on time and number of MT pulses, n , is illustrated in Fig. 1 for different values of PR. This experiment was carried out in WM with the strongest saturation applied during this study, i.e. an offset of 1 kHz and a nominal flip angle of 1440° . The display over time [Fig. 1(A)] shows the decrease of R_{app} at longer PR. On the other hand, a plot over the number of MT-pulses [Fig. 1(B)] shows that more MT pulses are required at shorter PR. The experimentally accessible parameter range is indicated by the data points. The closest approach to steady state (and hence the smallest errors in R_{app} and MTR) was achieved when applying all MT pulses during the maximum time. For PR = 40 ms, the steady state was reached by 98%. At longer PR, the steady state was not attainable due to slower transitions, at shorter PR due to a restriction in the number of MT pulses. Slower transitions were observed in GM, and also for weaker saturation at larger offsets or smaller flip angles (data not shown).

The MT-related increase of the fitted apparent saturations from δ_f to δ_{eq} with PR is shown in Fig. 2. The MT contributions were larger in WM due to its larger macromolecular content. When increasing the nominal flip angle from 1080 to 1260 and 1440° , δ_{eq} of WM increased from 5.7 ± 0.1 to 6.8 ± 0.2 and $7.6 \pm 0.2\%$, respectively. The corresponding values in GM were 4.0 ± 0.3 , 4.6 ± 0.2 and $5.2 \pm 0.2\%$. These values were reproduced with similar errors in different subjects. This also shows that the MT pulse was probably not able to fully saturate the macromolecular pool, as the changes in equilibrium saturation would be expected to become smaller when δ_m approached the limit of full saturation. The maximum MT effect was reached at PRs of about 100 ms in both

WM and GM. Specific values of λ_T cannot be given since an evaluation of all parameters in eqn (4) was not possible. The curves shown are an exponential approximation for large $\delta_m \approx 1$. Even at the shortest PR of 15 ms, δ_{app} was at least twice as large as δ_f .

Figure 3 illustrates the trade-off between direct saturation and MT effect by frequency offset. The relation between δ_{app} and δ_f was explored by comparing measurements at PR = 30 ms in WM (diamonds) and in a relaxation matched phantom (circles). The strong increase in the apparent saturation at offsets smaller than 2 kHz is accompanied by a rise in direct saturation. The contributions from MT as represented by the difference between the two values (solid squares) remain almost constant at such small offsets. Reducing the frequency offset first maximized the differential saturation and then led to higher direct contributions to δ_{app} . Thus, the band of direct saturation coincided roughly with the plateau of the much wider absorption lineshape of the macromolecules, although this finding may be specific for the applied MT pulse.

The apparent transition rate, R_{app} , decreased monotonously with PR (Fig. 4). This indicated that the PR-related increase in δ_{app} in brain tissue was too small to counteract the division by PR in eqn (9). The fitted values of R_{app} converged slowly onto the time dependence in the long-PR limit [eqn (10)]. By rapid pulsing, a faster transition to steady state was achieved. Since Fig. 3 indicates reduced MT at shorter PR, this is primarily due to repetitive direct saturation, but not due to MT.

No systematic differences between the relaxation factors, E_R , obtained with different MT pulses were observed. However, the error increased with PR and with lower saturation. By an error-weighted fit (Fig. 5) the apparent relaxation rates were determined as

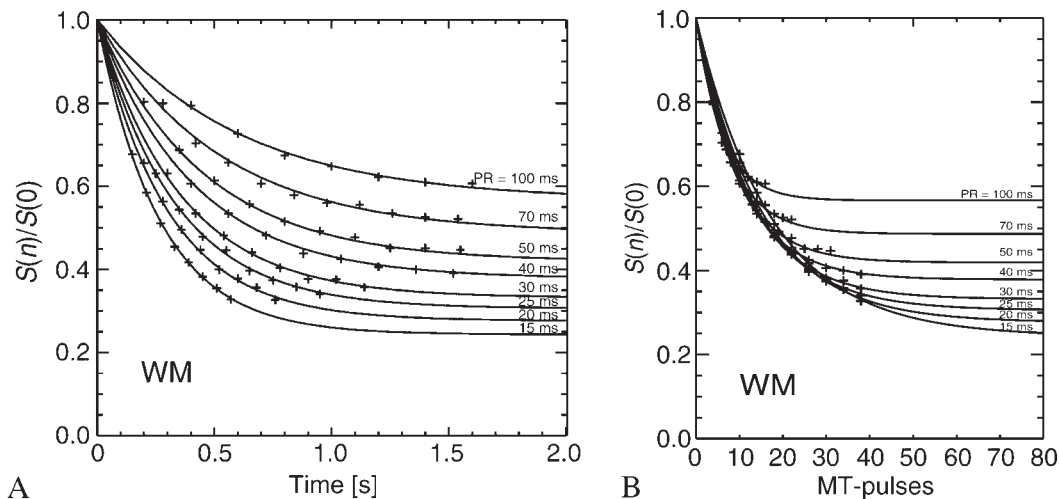


Figure 1. The transient behavior in WM measured at 1 kHz offset and 1440° amplitude. The normalized signal is displayed over time (A) and over number of MT pulses (B). The data points show the restrictions in time (1.6 s) and pulses (about 40). Note that for a shorter PR more pulses are needed to reach steady state as both $1 - \delta_{app}$ and E_R increase. However, the transition rate is faster because the direct saturation is applied more often

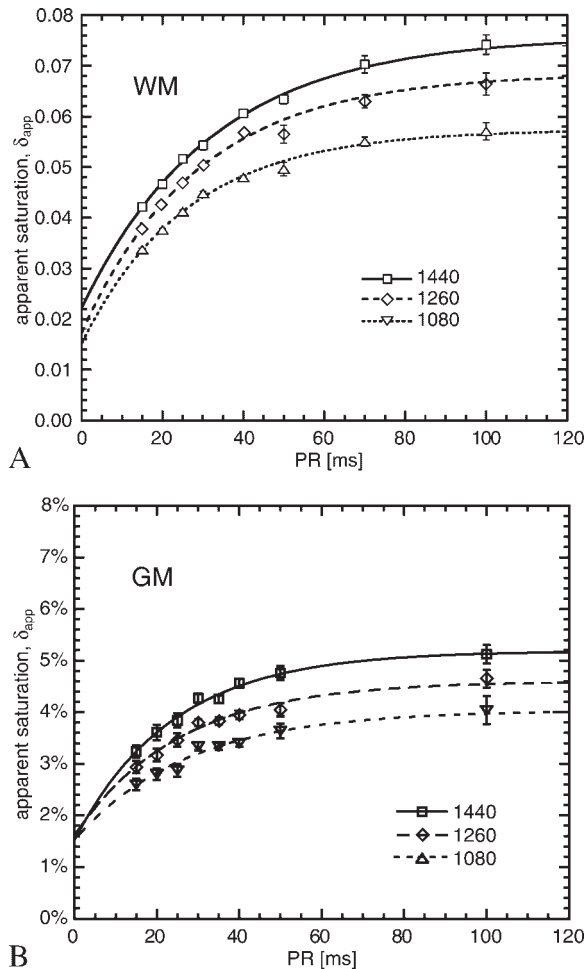


Figure 2. PR-dependence of the apparent saturation. Measurements in WM (A) and GM (B) are shown. MT pulses were applied at 1 kHz with nominal flip angles of 1080° (triangles), 1260° (diamonds) and 1440° (squares). The MT contributions to δ_{app} increase with PR. Increasing the nominal flip angle increases the differential saturation, $\delta_m - \delta_f$, and thus the MT contributions to δ_{app} . Since not all parameters of eqn (4) could be determined, an exponential PR-dependence, $\delta_{app} = \delta_{eq} + (\delta_f - \delta_{eq}) \exp(-PR/C)$, was fitted for visualization. The time constant C was about 30 ms in WM, and 25 ms in GM

$1.03 \pm 0.11 \text{ s}^{-1}$ in WM and $0.74 \pm 0.06 \text{ s}^{-1}$ in GM (mean \pm SD of six subjects). The reduction in free evolution by the MT pulse showed a large SD, but was on average less than one quarter of the pulse duration but subject to large errors ($2.3 \pm 2.9 \text{ ms}$ in WM, and $2.4 \pm 1.3 \text{ ms}$ in GM). No significant influence of different macromolecular fractions and exchange kinetics on ΔPR was found in GM and WM.

DISCUSSION

In this study, we applied repetitive MT pulses in order to estimate parameters describing saturation (δ_{app}) and re-

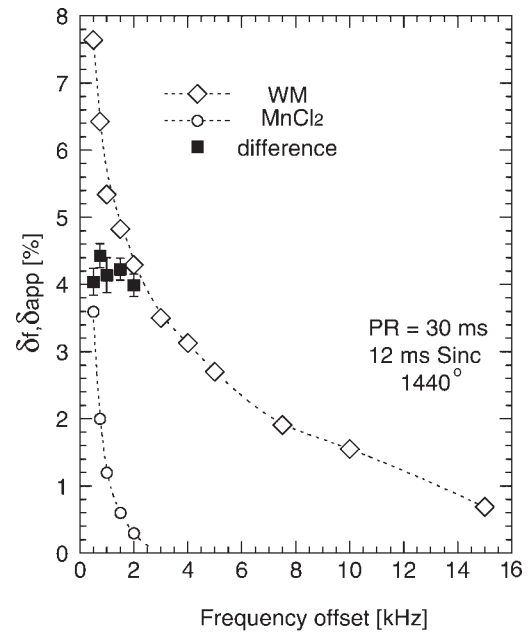


Figure 3. Trade-off between direct saturation and MT in WM by frequency offset. The strong increase in δ_{app} below 2 kHz is due to direct saturation as determined on a relaxation matched MnCl_2 solution. The difference—an estimate for the MT contributions—is almost constant in this frequency range. The error bars indicate the summed errors of the two independent measurements. At 0.5 kHz offset direct saturation and MT effect are almost equal

laxation (E_R) from the transition to the steady state. Such measurements require ‘single-shot’ sequences. A similar approach was used by Gochberg *et al.*, who estimated the macromolecular fraction from δ_{eq} of an ‘inverse MT’ experiment using multiple inversion pulses.¹² Their evaluation was based on somewhat stronger assumptions ($k_{mf} \gg k_{fm}, R_{1f}, R_{1m}$). We used a simplified description of pulsed MT that exploits the analogy between progressive saturation and the standard two-pool model for MT in tissues for the whole range of PR. This approximation is based on the combination of small macromolecular content and negligible difference in relaxation during the transfer time.⁹ The same approximations can be obtained from ‘indicator dilution theory’ with the additional assumption of $k_{mf} \gg R_{1f}, R_{1m}$.¹⁷ The theory of this article corrects our preliminary accounts,^{14,18,19} where we erroneously linearized E_T and neglected direct saturation. By assessing ΔPR we verified the assumption that the evolution is described by PR rather than by the interval without RF irradiation.^{3,9–12} Although the MT pulses, with some approximation, may be regarded as instantaneous, their influence on the evolution of the fast transfer component, E_T , is difficult to estimate. Shorter MT pulses are therefore recommended for quantitative evaluation to reduce this bias. Longitudinal relaxation rates derived from E_R were smaller than measured on spectroscopic volumes at 1.5 T.^{20,21} The partial saturation measurements on the MnCl_2 phantom also yielded a longer T_1

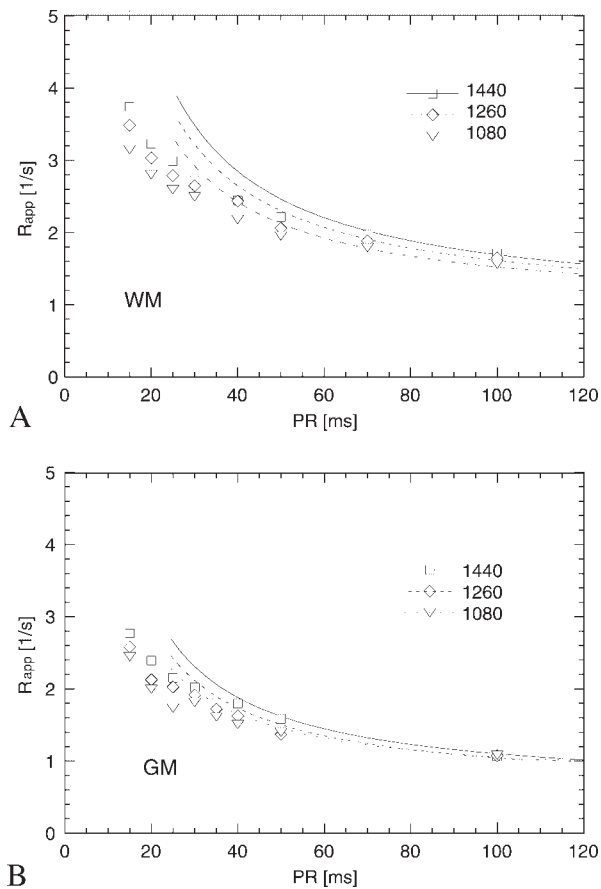


Figure 4. PR-dependence of the apparent transition rate, R_{app} . R_{app} decreases with PR, since the increase of δ_{app} is smaller than F . The decrease was stronger in WM (A) than in GM (B). The limit for negligible direct saturation at very long PR is λ_R . The curves depict the approximate behavior at long PR. The parameters of eqn (10) were determined from the measurements at PR = 100 ms

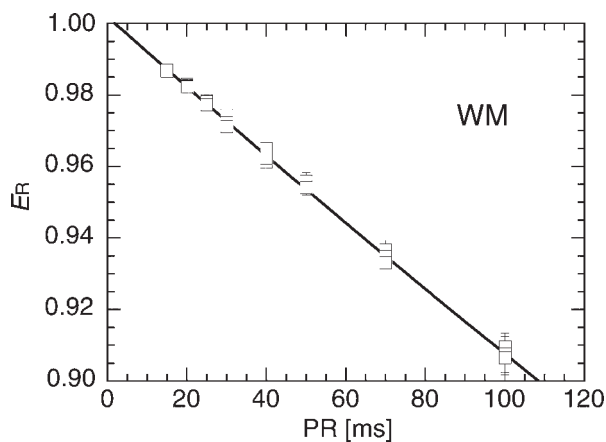


Figure 5. PR-dependence of the exponential factor. The two-parameter fit of eqn (11) yielded the apparent relaxation rate and a reduction in PR caused by the finite duration of the MT pulses. The E_R values and the data of Fig. 3(A) were derived from the same experiment

(729 ± 35 ms) than that measured by decreasing TR . A possible explanation is that the commonly used saturation method may be affected by inverse MT and partial saturation at the flanks of the profiles. The PRs were short compared with delays in conventional T_1 measurements. However, the findings cannot be explained by increased contributions from rapidly relaxing water moieties.

The ‘apparent saturation’ introduced in the theory section is particularly helpful in understanding the contributions of direct saturation and MT. The MT term in δ_{app} appears corrected for relaxation during PR. Therefore, it must not be confused with the term describing the time-evolution of the transferred amount of magnetization in a saturation transfer experiment. Because the latter is subject to relaxation, it shows a well-defined maximum at the critical delay.³ The MT term in δ_{app} increases with PR until both saturated pools are equilibrated at PRs longer than 100 ms in brain tissue. Its maximum is given by the product of macromolecular fraction and differential saturation. Comparison with F obtained by quantitative *in vivo* studies^{22–24} shows that the differential saturation was clearly below 100%. The transition of δ_{app} from δ_f to δ_{eq} is tissue specific, depending on the kinetic and relaxations rates. If the kinetic properties of MT are unknown, the transition has to be sampled at different PRs (Fig. 2). Thus, a phenomenological description of the PR-dependence of δ_{app} can be obtained. A quantification of all five parameters occurring in eqn (4) is possible when PR is sampled at both short values (like in this study) and long values (>100 ms).⁷

Our findings also suggest a strategy for optimizing the transition to steady state: first, the MT term of δ_{app} should be maximized. This should be achieved by means of a sufficiently long PR and by maximizing the differential saturation by increasing the pulse power at a frequency offset outside the band of direct excitation. If the number of MT pulses is limited, the transient may be reduced by increasing PR beyond 100 ms, where the maximum MT effect (δ_{eq}) is attained. This reduces the number of MT pulses at the cost of a slower transition and diminished steady state MTR [Fig. 1(A)]. If the total duration of the pulse train is limited, the number of pulses must be increased. This accelerates the transition rate at the cost of an inferior proportion between MT and direct saturation. This can be pursued until the limits of heat deposition or the RF power amplifier are reached. In this case, or if both time and number of pulses are limited, all available pulses should be applied in the available preparation time. The transition can be further accelerated by increasing the direct saturation. This is achieved by reducing the frequency offset.

In quantitative^{22–24} MT imaging, gradient-echo sequences have been used with PRs that were much shorter than 100 ms. This increases the weight of direct saturation because the MT contributions are not given enough time to develop. Since the MT term is always smaller

than the macromolecular fraction, the direct saturation should be always kept much smaller than F to avoid a dominance of direct saturation in the MTR.⁹ Hence, increasing the direct saturation by decreasing the frequency offset may not be an option if the macromolecular content is low, or if contributions from tissue to the apparent CSF component are to be identified.^{5,6} The theory of MT pulse trains does not apply to conventional MT spin-echo MRI, where the water magnetization is 'purged' during TR by the slice excitation. If a resonant saturation pulse before the pulse train is used to 'prepare' the bulk water into a state that is closer to the steady state than the equilibrium, fewer pulses will be needed to close up on the steady state. This may be exploited to shorten the transition. However, if the CSF signal of the single-shot read-out is suppressed by inversion recovery, the transfer of saturation from the free to the macromolecular pool ('inverse MT') has to be taken into account.

The strategy to derive λ_R and δ_{app} from the transient progressive saturation allows to use δ_{app} as an estimate for MT that is not confounded by differences in relaxation. However, this requires similar degrees of saturation in different brain regions. This was confirmed for normal brain in our proof-of-principle study⁷ and by other quantitative studies that yielded similar T_{2m} values for grey and white matter.^{22–24} Mapping of the whole brain is possible by performing echo-planar imaging with a suitable permutation of slice order. Since specific heat absorption is not an issue, this strategy is suitable also for field strengths of 3 T and higher.

CONCLUSIONS

When using equidistant trains of MT pulses, the transition to steady state can be described by two different parameters: the longitudinal relaxation during PR and the apparent degree of saturation. The latter is a measure for MT that is not confounded by relaxation. The transition to steady state is always faster than given by apparent relaxation of the water. To maximize MT contributions, the differential saturation created by the MT pulse should be optimized and the repetition period of the MT pulses in brain should be about 100 ms. The offset may be increased to 2.5 kHz to reduce direct saturation without sacrificing MT in white matter. The transition can be accelerated by reducing PR or reducing the frequency offset. Even though larger MTRs are observed, this increases relative contributions from direct saturation.

REFERENCES

- Wolff SD, Balaban RS. Magnetization transfer contrast (MTC) and tissue water proton relaxation *in vivo*. *Magn. Reson. Med.* 1989; **10**: 135–144.
- Edzes HT, Samulski ET. The measurement of cross-relaxation effects in the proton NMR spin-lattice relaxation of water in biological systems: hydrated collagen and muscle. *J. Magn. Reson.* 1978; **31**: 207–229.
- Graham SJ, Henkelman RM. Understanding pulsed magnetization transfer. *J. Magn. Reson. Imag.* 1997; **7**: 903–912.
- Helms G, Frahm J. Magnetization transfer attenuation of creatine resonances in localized proton MRS of human brain *in vivo*. *NMR Biomed.* 1999; **12**: 490–494.
- Helms G, Piringer A. Magnetization transfer of water T_2 relaxation components in human brain: implications for T_2 -based segmentation of spectroscopic volumes. *Magn. Reson. Imag.* 2001; **19**: 803–811.
- Helms G. T_2 -based segmentation of periventricular spectroscopic volumes for quantification of proton MR spectra of multiple sclerosis lesions. *MAGMA* 2003; **19**: 10–16.
- Helms G, Hagberg GE. Quantification of magnetization transfer by sampling the transient signal using MT-prepared single-shot EPI. *Concepts Magn. Reson. A* 2003; **19A**: 149–153.
- Roell SA, Dreher W, Leibfritz D. Combining CW and pulsed saturation allows *in vivo* quantification of magnetization transfer observed for total creatine by ^1H -NMR-spectroscopy of rat brain. *Magn. Reson. Med.* 1999; **42**: 222–227.
- Helms G, Hagberg GE. Pulsed saturation of the standard two-pool model for magnetization transfer—Part I: the steady state. *Concepts Magn. Reson. A* 2004; **21A**: 37–49.
- Helms G, Dathe H, Hagberg GE. Pulsed saturation of the standard two-pool model for magnetization transfer—Part II: the transition to steady state. *Concepts Magn. Reson. A* 2004; **21A**: 50–61.
- Pike GB. Pulsed magnetization transfer contrast in gradient echo imaging: a two-pool analytic description of the signal response. *Magn. Reson. Med.* 1996; **36**: 95–103.
- Gochberg DF, Kennan RP, Robson MD, Gore JC. Quantitative imaging of magnetization transfer using multiple selective pulses. *Magn. Reson. Med.* 1999; **41**: 1065–1072.
- Frahm J, Merboldt KD, Hänicke W. Localized proton spectroscopy using stimulated echoes. *J. Magn. Reson.* 1987; **72**: 502–505.
- Piringer A. Quantitative evaluation of magnetisation transfer in human brain: extrapolation from fast pulse repetition to continuous wave saturation. M.Sc. thesis. Medical Radiation Physics, Stockholm University, 1998.
- Henkelman RM, Stanisz GJ, Graham SJ. Magnetisation transfer in MRI: a review. *NMR Biomed.* 2001; **14**: 57–64.
- Berry I, Barker GJ, Barkhof F, Campi A, Dousset V, Franconi J-M, Gass A, Schreiber W, Miller DH, Tofts PS. A multicenter measurement of magnetization transfer ratio in normal white matter. *J. Magn. Reson. Imag.* 1999; **9**: 441–446.
- Ropele S, Seifert T, Enzinger C, Fazekas F. Method for quantitative imaging of the macromolecular ^1H fraction in tissue. *Magn. Reson. Med.* 2003; **49**: 864–871.
- Piringer A, Helms G. Quantitative magnetization transfer in human brain: extrapolation from fast pulse repetition to CW saturation. In *Book of Abstracts, 6th Annual Meeting of the International Society of Magnetic Resonance in Medicine*. ISMRM: Berkeley CA, 1998; 2191.
- Helms G, Piringer A. Dynamic evaluation of magnetization transfer in human brain: the approach to steady state after pulsed saturation. In *Book of Abstracts, 6th Annual Meeting of the International Society for Magnetic Resonance in Medicine*. ISMRM: Berkeley CA, 1998; 2192.
- Brief EE, Whittall KP, Li DKB, MacKay AL. Proton T_1 relaxation times of cerebral metabolites differ within and between regions of normal human brain. *NMR Biomed.* 2003; **16**: 503–509.
- Ethofer T, Mader I, Seeger U, Helms G, Erb M, Grodd W, Ludolph A, Klose U. Comparison of longitudinal metabolite relaxation times in different regions of the human brain at 1.5 and 3 Tesla. *Magn. Reson. Med.* 2003; **50**: 1296–1301.
- Sled JG, Pike GB. Quantitative imaging of magnetization transfer exchange and relaxation properties *in vivo* using MRI. *Magn. Reson. Med.* 2001; **46**: 923–931.
- Yarnykh VL. Pulsed Z-spectroscopic imaging of cross-relaxation parameters in tissues for human MRI: theory and clinical applications. *Magn. Reson. Med.* 2002; **47**: 929–939.
- Ramani A, Dalton C, Miller DH, Tofts PS, Barker GJ. Exact estimation of MT parameters in human brain in clinically feasible times. *Magn. Reson. Imag.* 2002; **20**: 721–731.